

# A Partial Initialization Strategy to Mitigate the Overfitting Problem in CATE Estimation with Hidden Confounding

Chuan Zhou\*  
zhouchuan@pku.edu.cn  
Peking University & MBZUI  
Beijing, China

Yaxuan Li\*<sup>†</sup>  
yaxuanli.cn@gmail.com  
Peking University  
Beijing, China

Chunyuan Zheng  
cyzheng@stu.pku.edu.cn  
Peking University & MBZUI  
Beijing, China

Haiteng Zhang  
zhanghaiteng22@mails.ucas.ac.cn  
Chinese Academy of Sciences &  
MBZUI  
Beijing, China

Haoxuan Li<sup>‡</sup>  
hxli@stu.pku.edu.cn  
Peking University & MBZUI  
Beijing, China

Mingming Gong<sup>‡</sup>  
mingming.gong@unimelb.edu.au  
The University of Melbourne &  
MBZUI  
Melbourne, Australia

## Abstract

Estimating the conditional average treatment effect (CATE) from observational data plays a crucial role in areas such as e-commerce, healthcare, and economics. Existing studies mainly rely on the strong ignorability assumption that there are no hidden confounders, whose existence cannot be tested from observational data and can invalidate any causal conclusion. In contrast, data collected from randomized controlled trials (RCT) do not suffer from confounding but are usually limited by a small sample size. To avoid overfitting caused by the small-scale RCT data, we propose a novel two-stage pretraining-finetuning (TSPF) framework with a partial parameter initialization strategy to estimate the CATE in the presence of hidden confounding. In the first stage, a foundational representation of covariates is trained to estimate counterfactual outcomes through large-scale observational data. In the second stage, we propose to train an augmented representation of the covariates, which is concatenated with the foundational representation obtained in the first stage to adjust for the hidden confounding. Rather than training a separate network from scratch, part of the prediction heads are initialized from the first stage. The superiority of our approach is validated on two datasets with extensive experiments.

## CCS Concepts

• Computing methodologies → Machine learning approaches.

## Keywords

Causal Effect Estimation, hidden Confounding, Data Fusion

\*Both authors contributed equally to this research.

<sup>†</sup>This work was done during the research internship of Yaxuan Li at Peking University.

<sup>‡</sup>Haoxuan Li and Mingming Gong are corresponding authors.

Permission to make digital or hard copies of all or part of this work for personal or classroom use is granted without fee provided that copies are not made or distributed for profit or commercial advantage and that copies bear this notice and the full citation on the first page. Copyrights for components of this work owned by others than the author(s) must be honored. Abstracting with credit is permitted. To copy otherwise, or republish, to post on servers or to redistribute to lists, requires prior specific permission and/or a fee. Request permissions from [permissions@acm.org](mailto:permissions@acm.org).

*CMLKDD2024, KDD 2024 Workshop, August 2024, Barcelona, Spain*

© 2024 Copyright held by the owner/author(s). Publication rights licensed to ACM.

ACM ISBN 978-1-4503-XXXX-X/18/06

<https://doi.org/XXXXXXX.XXXXXXX>

## ACM Reference Format:

Chuan Zhou, Yaxuan Li, Chunyuan Zheng, Haiteng Zhang, Haoxuan Li, and Mingming Gong. 2024. A Partial Initialization Strategy to Mitigate the Overfitting Problem in CATE Estimation with Hidden Confounding. In *CMLKDD2024: KDD 2024 Workshop, Aug 25–29, 2024, Barcelona, Spain*. ACM, New York, NY, USA, 7 pages. <https://doi.org/XXXXXXX.XXXXXXX>

## 1 Introduction

The conditional average treatment effect (CATE) is the average causal effect of a treatment or an intervention on the outcome of interest given the covariates [34], which plays an important role in diverse fields, such as trustworthy artificial intelligence [31], electronic commerce [42], healthcare [36], and economics [18]. In e-commerce, the platforms desire to predict how recommending a specific product to a particular user affects the probability of purchase [32], and thereby influence the total profit. In healthcare, doctors assess the potential outcome for different patient groups when receiving a certain treatment [7] for precision medicine. Similarly in economics, the policymakers evaluate how much a job training program will raise employment opportunities for certain groups of unemployed individuals [3].

To enhance the accuracy of CATE estimation, representation-based learning approaches have gathered increasing attention due to their impressive performance [21, 28, 40, 49]. These approaches focus on generating covariate representations, to mitigate confounding bias by minimizing distributional discrepancies between the treatment and control groups. Previous approaches have developed substantial theory and explored extensive practice to obtain such representations. For instance, some of them use integral probability metric (IPM) for regularization [21], while a few approaches emphasize local similarity preservation [44], targeted learning [47], or view the problem from new perspectives like optimal transport [40] and out-of-distribution [27].

However, the aforementioned methods may ignore hidden confounding, which is very common in real-world scenarios [29]. In our e-commerce example, the financial status of users might be sensitive and difficult to collect [30]. In the healthcare case, the personal lifestyles of patients are difficult to obtain [4]. For the example in economics, personal working status is difficult to measure [43]. These hidden variables can affect treatment and outcome simultaneously, which causes confounding bias in the estimation

of causal effects. Therefore, proposing methods to account for the confounding bias is crucial to accurately estimate CATE.

To address the hidden confounding problem, one category of mainstream methods can rely only on large-scale observational (OBS) data, including sensitivity analysis [8, 19], front-door adjustment methods [10], and instrumental variables methods [22]. These methods require additional strong assumptions that cannot be tested from the data and raise concerns if these assumptions are violated [11, 25]. Compared to the OBS data, randomized controlled trial (RCT) data are considered as the gold standard for causal effect estimation [35]. However, practical challenges such as high costs and ethical concerns may make the collection of RCT data difficult [2, 46], resulting in limited sample sizes. Due to the small size, it is impractical to directly train causal effect prediction models on RCT data alone [17]. Therefore, it is necessary to find an effective method to combine small-scale RCT data with large-scale OBS data. However, previous methods either rely on untestable strong assumptions [14, 23] or suffer from the risk of overfitting due to limited RCT sample sizes [6, 41].

In this paper, we introduce a two-stage pretraining-finetuning (TSPF) framework with a partial initialization strategy for CATE estimation under hidden confounding. Our approach leverages large-scale OBS data to train a foundational representation of covariates and then uses relatively small-scale RCT data to adjust the bias in the representation learned from OBS data. We then train an unbiased prediction model using this adjusted representation. In the second stage, we introduce an additional module that ensures stronger representation ability compared to the methods that use RCT data to estimate the residuals and initialize part of the prediction heads with parameters from the first stage.

The contributions of this paper are summarized as follows.

- We present the TSPF framework that includes a partial initialization strategy for CATE estimation, tackling hidden confounding by using a small amount of unconfounded RCT data to adjust the representations learned from OBS data.
- The proposed framework does not rely on the linear and additive generation assumptions, and can flexibly adjust its model structure according to the sample size of RCT data, thus mitigating the over-fitting problem.
- Experiments conducted on the semi-synthetic IHDP and Jobs datasets demonstrate the effectiveness of our approach.

## 2 Preliminaries

### 2.1 Problem Setup

We consider two independent data sources taken from the same target population: one from OBS and the other from RCT. Each individual in the OBS or RCT study is an observation of  $(X, Y, T, G)$ , a random tuple with distribution  $P$ . For the  $i$ -th individual, the observation comprises  $d$ -dimensional covariates  $X_i \in \mathcal{X} \subseteq \mathbb{R}^d$ , the observed outcome  $Y_i$ , the assigned binary treatments  $T_i \in \{0, 1\}$  ( $T_i = 0$  for the controlled and  $T_i = 1$  for the treated individuals) and  $G_i$  denoting participation in the OBS ( $G_i = 0$ ) or RCT ( $G_i = 1$ ) study. Using the Neyman-Rubin potential outcome framework [20], we let  $Y_i^1, Y_i^0$  be the potential outcomes. We denote the OBS data as  $\mathcal{D}^{OBS} = \{(X_i, T_i, Y_i, G_i = 0) : i \in \mathcal{O}\}$  with sample size  $n$ , and the RCT data as  $\mathcal{D}^{RCT} = \{(X_i, T_i, Y_i, G_i = 1) : i \in \mathcal{R}\}$  with sample size

$m$ , where  $\mathcal{O} = \{1, \dots, n\}$  and  $\mathcal{R} = \{n+1, \dots, n+m\}$  are sample index sets for the OBS and RCT data, respectively. The total sample size is  $N = n + m$ . We define the propensity score as  $e(x, G) = P(T = 1 | X = x, G)$ . The CATE is defined as the conditional expectation of difference between potential outcomes under the treatment group and the control group as follows:

$$\tau(x) = \mathbb{E}[Y^1 - Y^0 | X = x].$$

### 2.2 Identification of CATE

To identify the CATE from observed data, in addition to the Stable Unit Treatment Value Assumption (SUTVA) that there are no interference between units and there are no different forms of each treatment level, the following three assumptions are required:

**Assumption 1. (Ignorability)**  $(Y^1, Y^0) \perp\!\!\!\perp T | X$ ,

**Assumption 2. (Consistency)**  $Y = TY^1 + (1 - T)Y^0$ ,

**Assumption 3. (Positivity)**  $0 < e(x, G = 1) < 1$ .

Assumption 1 is also known as no hidden confounding, which holds in the RCT by default due to the randomized treatment assignment. We can identify CATE based on the RCT data:

$$\tau(x) = \mathbb{E}[Y | T = 1, X = x, G = 1] - \mathbb{E}[Y | T = 0, X = x, G = 1].$$

The unconfoundedness assumption is not assumed to hold for the observational data, i.e.  $(Y^1, Y^0) \not\perp\!\!\!\perp T | (X, G = 0)$ . We cannot identify  $\tau(x)$  based on OBS data only. Let us denote the difference in conditional average outcomes in the observational data by:

$$\zeta(x) = \mathbb{E}[Y | T = 1, X = x, G = 0] - \mathbb{E}[Y | T = 0, X = x, G = 0].$$

Note that due to hidden confounding,  $\zeta(x) \neq \tau(x)$  for any  $x$ . The difference between these two quantities is precisely the confounding effect, which we denote the residual function as:

$$\eta(x) = \tau(x) - \zeta(x).$$

## 3 Methodology

In this section, we present a two-stage framework for the estimation of CATE based on the pretraining-finetuning principle, as shown in Figure 1. The motivation is to use large-scale OBS data to train a foundational representation of covariates, then to use relatively small-scale unbiased RCT data to remove the bias in the representation learned from OBS data for training the unbiased prediction model. Specifically, in the first stage, only the OBS data is used. We start with a representation module  $\phi$ , followed by one reconstruction module  $\psi$  and two prediction heads  $h_0$  and  $h_1$  to ensure the learned covariate representation can have enough information and predict the outcome for control group and treatment group simultaneously. While in the second stage, we use only the RCT data. The representation module  $\phi$  learned in the first stage is frozen, with a learnable representation adapter module  $\phi^U$  to remove the bias of  $\phi$ . Then the concatenated representation is fed to two prediction heads  $g_0$  and  $g_1$  to obtain the unbiased predicted potential outcomes under control and treatment groups respectively. We carefully design an initialization strategy to ensure that the initialized second-stage model produces the same predictions as the converged model in the first stage. Our approach distinguishes from the one proposed by Kallus et al. [23], which only uses linear regression to estimate the

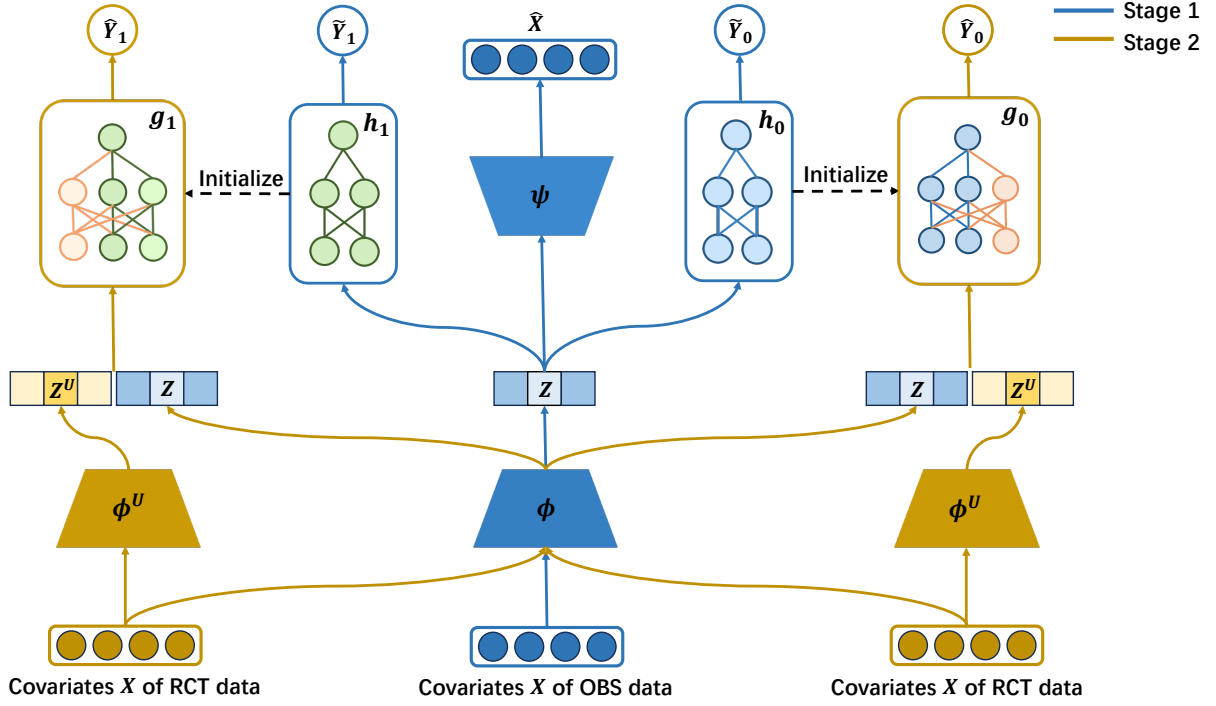


**Figure 1: The framework of our proposed method, composed of the modules for the first stage (blue) and second stage (yellow). Note that the two  $\phi^U$  shown in the figure represent the same module.**

residual function  $\eta(x)$  in the second stage. We can regard the first stage as pretraining on the large OBS data and the second stage as finetuning on the small-scale unbiased RCT data.

### 3.1 First Stage: Pretraining Stage

The goal of our first-stage training is to obtain a representation module as well as prediction heads that can accurately estimate the potential outcomes of OBS data. These modules offer high-quality initialization for second-stage training, allowing fine-tuning on the RCT data to avoid the overfitting problem. A three-headed architecture and a multi-task training framework are employed to achieve this goal. Next, we will look into the details of each module.

**3.1.1 Representation.** We design a multi-layer feed-forward neural network  $\phi$  to obtain a representation  $Z$  for the covariates  $X$  for both treatment and control groups. In other words, for an individual sample  $(X_i, T_i, Y_i, G_i = 0)$ , the representation  $Z_i = \phi(X_i)$  remains the same whether  $T_i = 0$  or  $T_i = 1$ . To better estimate the causal effect, we adopt the idea of covariate balancing on the representation space as Shalit et al. [37]. Specifically, the representations for treatment group  $\{Z_i = \phi(X_i) : G_i = 0, T_i = 1\}$  are regarded as i.i.d samples drawn randomly from a distribution  $P_\phi^{t=1}$  and similarly  $P_\phi^{t=0}$  for the control group. We anticipate the distributions of representations to be similar between the treatment and control groups. An integral probability metric (IPM) is employed to measure the distance between the two distributions. Thus the covariate

unbalancing loss is defined as:

$$\mathcal{L}_{unb} = \text{IPM}_{\mathcal{G}}(\hat{P}_\phi^{t=1}, \hat{P}_\phi^{t=0}),$$

where  $\text{IPM}_{\mathcal{G}}(\cdot)$  is the empirical IPM defined by the function family  $\mathcal{G}$ , and  $\hat{P}_\phi^{t=1}$  and  $\hat{P}_\phi^{t=0}$  are empirical distributions of  $P_\phi^{t=1}$  and  $P_\phi^{t=0}$  respectively. In the implementation, we adopt the Wasserstein distance as a showcase, which can be consistently estimated from finite samples within a mini-batch [9].

**3.1.2 Reconstruction and Prediction.** To ensure that  $Z$  retains as much information about the original covariates as possible, we introduce the decoder network  $\psi$  to reconstruct the original covariates:  $\hat{X} = \psi(Z) = \psi(\phi(X))$ . The reconstruction loss is computed by the mean squared error (MSE):

$$\mathcal{L}_{rec} = \frac{1}{|\mathcal{O}|} \sum_{i \in \mathcal{O}} \|\hat{X}_i - X_i\|_2^2,$$

where  $\hat{X}_i = \psi(\phi(X_i))$  is reconstructed covariate for the  $i$ -th sample in the OBS data. The reconstruction design resembling an autoencoder allows the learned representations to encompass nearly complete information in the covariates, rather than only the information necessary for fitting the training set, thereby enhancing the generalization of our representation module.

We then use the representations  $Z$  to estimate the potential outcomes with two  $l_p$ -layer prediction heads  $h_0$  and  $h_1$ , which are the predictors for control and treatment outcomes, respectively.

Note that hidden confounding in the observational data can lead to biased estimations of potential outcomes, we refer to the prediction result  $\hat{Y}^0 = h_0(Z) = h_0(\phi(X))$  as the pseudo control outcome and  $\hat{Y}^1 = h_1(Z) = h_1(\phi(X))$  as the pseudo treatment outcome. To enhance comparability between the treatment group and control group, we employ a reweighting technique to balance the two groups. Formally, let  $f_h(x, t) = h_t(\phi(x))$  with  $t \in \{0, 1\}$  be the predicted potential outcomes by via the two heads  $h_0$  and  $h_1$ , the loss for outcome prediction is as follows:

$$\mathcal{L}_f = \frac{1}{|\mathcal{O}|} \sum_{i \in \mathcal{O}} w_i \cdot l(Y_i, f_h(X_i, T_i)),$$

with  $w_i = \frac{T_i}{2u} + \frac{1-T_i}{2(1-u)}$ , where  $u = \frac{1}{n} \sum_{i=1}^n T_i$ . The loss function  $l(\cdot, \cdot)$  in  $\mathcal{L}_f$  is flexible and can be determined based on the value range of potential outcomes. If the potential outcomes are binary, a cross-entropy loss is appropriate, whereas for continuous potential outcomes, an MSE loss is preferable.

In summary, in the first-stage training, we use the following training objective:

$$\min_{\phi, \psi, h_0, h_1} \mathcal{L}_f + \lambda_1 \mathcal{L}_{rec} + \lambda_2 \mathcal{L}_{unb},$$

where  $\lambda_1 > 0$  and  $\lambda_2 > 0$  are tunable hyperparameters.

### 3.2 Second Stage: Finetuning Stage

In the second stage of training, we exploit the small-scale unconfounded RCT data to remove the hidden confounding by concatenating the learned covariate representation in the first stage with a newly learned augmented covariate representation, then finetuning the prediction heads to obtain an unbiased CATE estimation. To achieve this, we keep the biased representation  $Z$  produced by  $\phi$  unchanged but only treat it as a part of the representation, together with an additional  $Z^U$  generated by another representation module  $\phi^U$ . We call  $\phi^U$  a representation adapter, as it helps to adapt the final representation to account for the hidden confounding in the observed data. In addition, a large proportion of the parameters of the prediction heads  $g_0$  and  $g_1$  are initialized by  $h_0$  and  $h_1$ , respectively. With the above steps, the second stage aims at adjusting the hidden confounding through the augmented covariate representation and the finetuned prediction heads with partial parameter initialization. Below we explain the modules in detail.

**3.2.1 Representation Adapter.** We employ a shallower feed-forward network  $\phi^U$  as the representation adapter. It is worth noting that the width and depth of  $\phi^U$  can be adjusted based on the scale of RCT data size. If the size of RCT data was comparable to that of OBS data, we can use the same architecture as  $\phi$ . However, in real-world cases, the RCT data is rare compared to the OBS data, so the size of  $\phi^U$  should be smaller. We denote the representation generated by  $\phi^U$  as  $Z^U$ . To make sure that  $Z^U$  captures different features of covariates from  $Z$ , we employ mutual information to control the overlap between the two covariate representations:

$$\mathcal{L}_{MI} = CLUB(Z, Z^U),$$

$$\begin{aligned} CLUB(Z, Z^U) &= \frac{1}{m^2} \sum_{i \in \mathcal{R}} \sum_{j \in \mathcal{R}} \left[ \log q_\theta(Z_i^U | Z_i) - \log q_\theta(Z_j^U | Z_i) \right] \\ &= \frac{1}{m} \sum_{i \in \mathcal{R}} \left[ \log q_\theta(Z_i^U | Z_i) - \frac{1}{m} \sum_{j \in \mathcal{R}} \log q_\theta(Z_j^U | Z_i) \right], \end{aligned}$$

where  $CLUB(Z, Z^U)$  is the empirical Contrastive Log-ratio Upper Bound (CLUB) of mutual information [5] between two covariate representations  $Z$  and  $Z^U$ , and  $q_\theta(Z^U | Z)$  is the variational approximation of  $P(Z^U | Z)$ . With good variational approximation  $q_\theta(Z^U | Z)$ , it can be shown that the empirical CLUB is still a valid upper bound of the ground-truth mutual information.

**3.2.2 Prediction.** Similarly to the first stage, we design two  $l_p$ -layer prediction heads  $g_0$  and  $g_1$  to estimate the potential outcomes under control and treatment groups with hidden confoundings, respectively. Notice that  $g_0, g_1$  and  $h_0, h_1$  have the same depth  $l_p$ , yet every layer of  $g_t$  has a larger or equal width than  $h_t$ . For  $t \in \{0, 1\}$ , we define the header  $h_t$  as:

$$\begin{aligned} a_{h_t}^{(0)} &= Z, \quad a_{h_t}^{(l)} = \sigma(W_{h_t}^{(l)} a_{h_t}^{(l-1)} + b_{h_t}^{(l)}), \quad \text{for } l = 1, 2, \dots, l_p - 1, \\ a_{h_t}^{(l_p)} &= \hat{Y}_t = W_{h_t}^{(l_p)} a_{h_t}^{(l_p-1)} + b_{h_t}^{(l_p)}, \end{aligned}$$

where  $W_{h_t}^{(l)}$  is the weight matrix from layer  $l-1$  to layer  $l$ ,  $b_{h_t}^{(l)}$  is the bias vector of layer  $l$ ,  $a_{h_t}^{(l)}$  is the output of layer  $l$  for  $l \in \{1, 2, \dots, l_p\}$  and  $\sigma$  is the activation function. The definition of  $g_t$  is:

$$\begin{aligned} a_{g_t}^{(0)} &= \begin{bmatrix} Z \\ Z^U \end{bmatrix}, \quad a_{g_t}^{(l)} = \sigma(W_{g_t}^{(l)} a_{g_t}^{(l-1)} + b_{g_t}^{(l)}), \quad \text{for } l = 1, 2, \dots, l_p - 1, \\ a_{g_t}^{(l_p)} &= \hat{Y}_t = W_{g_t}^{(l_p)} a_{g_t}^{(l_p-1)} + b_{g_t}^{(l_p)}, \end{aligned}$$

with  $W_{g_t}^{(l)}, b_{g_t}^{(l)}, a_{g_t}^{(l)}$  having similar meanings as  $W_{h_t}^{(l)}, b_{h_t}^{(l)}, a_{h_t}^{(l)}$  but for  $g_t$ ,  $\hat{Y}_t$  is the final prediction for potential outcome under treatment  $t$ . In our design, every layer of  $g_t$  has a larger or equal width than  $h_t$ , thus the dimension of  $W_{g_t}^{(l)}, b_{g_t}^{(l)}, a_{g_t}^{(l)}$  is no less than that of  $W_{h_t}^{(l)}, b_{h_t}^{(l)}, a_{h_t}^{(l)}$ , respectively. We divide the parameters of  $g_t$  as:

$$W_{g_t}^{(l)} = \begin{bmatrix} 1 W_{g_t}^{(l)}, 2 W_{g_t}^{(l)} \\ 3 W_{g_t}^{(l)}, 4 W_{g_t}^{(l)} \end{bmatrix}, \quad b_{g_t}^{(l)} = \begin{bmatrix} 1 b_{g_t}^{(l)} \\ 2 b_{g_t}^{(l)} \end{bmatrix},$$

where  ${}^1 W_{g_t}^{(l)}, {}^1 b_{g_t}^{(l)}$  have the same shapes as  $W_{h_t}^{(l)}, b_{h_t}^{(l)}$  respectively, for  $l = 1, 2, \dots, l_p$ , with the detailed initialization strategy as follows.

**Initialization.** The initialization of the model parameters is crucial for the preservation of covariate information from the first stage as well as the effectiveness of the finetuning stage. The goal of initialization is to make sure the model initially produces the same prediction as the trained first-stage model. Nonetheless, a challenge of parameter initialization is that the model architecture of the second stage differs from that of the first stage, because of the augmented covariate representation. Based on the division of the parameters, we propose the following initialization strategy:

$$({}^1 W_{g_t}^{(l)}, {}^2 W_{g_t}^{(l)}, {}^3 W_{g_t}^{(l)}, {}^4 W_{g_t}^{(l)}, {}^1 b_{g_t}^{(l)}, {}^2 b_{g_t}^{(l)}) \leftarrow (W_{h_t}^{(l)}, 0, 0, 0, b_{h_t}^{(l)}, 0)$$

for  $l = 1, 2, \dots, l_p$ . That is, the shared parameters between the prediction heads  $g_t$  and  $h_t$  are initialized to be the same, and the rest parameters of the prediction head  $g_t$  are initialized to be zero.

**Algorithm 1:** Learning algorithm of the TSPF framework.

---

**Input:** OBS data  $\mathcal{D}^{OBS} = \{(X_i, T_i, Y_i, G_i = 0)\}_{i=1}^n$ , RCT data  $\mathcal{D}^{RCT} = \{(X_i, T_i, Y_i, G_i = 1)\}_{i=n+1}^{n+m}$  and four hyperparameters  $\lambda_k > 0, k = 1, \dots, 4$ .  
 Compute  $w_i = \frac{T_i}{2u} + \frac{1-T_i}{2(1-u)}$  with  $u = \frac{1}{n} \sum_{i=1}^n T_i$  for  $i = 1, \dots, n$ ;  
**for** number of steps for training the first-stage model **do**  
   Sample a batch  $\{(X_i, T_i, Y_i)\}_{i \in B}$  from  $\mathcal{D}^{OBS}$ ;  
   Update  $\theta_1 = (\theta_\phi, \theta_\psi, \theta_{h_0}, \theta_{h_1})$  by descending along the gradient  $\nabla_{\theta_1} (\mathcal{L}_f + \lambda_1 \mathcal{L}_{rec} + \lambda_2 \mathcal{L}_{unb})$ ;  
**end**  
 Initialize  $({}^1W_{g_t}^{(l)}, {}^2W_{g_t}^{(l)}, {}^3W_{g_t}^{(l)}, {}^4W_{g_t}^{(l)}, {}^1b_{g_t}^{(l)}, {}^2b_{g_t}^{(l)})$  by  $(W_{h_t}^{(l)}, 0, 0, 0, b_{h_t}^{(l)}, 0)$  for  $l = 1, 2, \dots, l_p$  and  $t = 0, 1$ ;  
 Compute  $w_i = \frac{T_i}{2u} + \frac{1-T_i}{2(1-u)}$  with  $u = \frac{1}{m} \sum_{i=n+1}^{n+m} T_i$  for  $i = n+1, \dots, n+m$ ;  
**for** number of steps for training the second-stage model **do**  
   Sample a batch  $\{(X_i, T_i, Y_i)\}_{i \in B}$  from  $\mathcal{D}^{RCT}$ ;  
   Update  $\theta_2 = (\theta_{\phi^U}, \theta_{g_0}, \theta_{g_1})$  by descending along the gradient  $\nabla_{\theta_2} (\mathcal{L}_{pred} + \lambda_3 \mathcal{L}_{MI} + \lambda_4 \mathcal{L}_{shift})$ ;  
**end**

---

As in the first stage, we denote  $f_g(x, t) = g_t([\phi(x)^\top | \phi^U(x)^\top]^\top)$  for  $t \in \{0, 1\}$ , where  $[\phi(x)^\top | \phi^U(x)^\top]$  is the concatenated covariate representation. Given the RCT data  $\{(X_i, T_i, Y_i, G_i = 1) : i \in \mathcal{R}\}$ , the prediction loss is computed as:

$$\mathcal{L}_{pred} = \frac{1}{|\mathcal{R}|} \sum_{i \in \mathcal{R}} w_i \cdot l(Y_i, f_g(X_i, T_i)),$$

similarly with  $w_i = \frac{T_i}{2u} + \frac{1-T_i}{2(1-u)}$  and  $u = \frac{1}{m} \sum_{i=n+1}^{n+m} T_i$ .

*Regularization.* Since small-scale RCT data may cause overfitting during the finetuning phase, we further introduce a constraint to ensure that the parameters of the second-stage finetuned model do not deviate significantly from the parameters of the first-stage trained model. Denote the initial value of  $\theta_{g_t}$  as  $\theta_{g_t}^0$ , to constrain the deviation from the initial value, we propose to use  $l_2$ -norms in the training loss objective:

$$\mathcal{L}_{shift} = \|\theta_{g_0} - \theta_{g_0}^0\|_2^2 + \|\theta_{g_1} - \theta_{g_1}^0\|_2^2.$$

Overall, the training loss of the second stage is given by:

$$\min_{\phi^U, g_0, g_1} \mathcal{L}_{pred} + \lambda_3 \mathcal{L}_{MI} + \lambda_4 \mathcal{L}_{shift},$$

where  $\lambda_3$  and  $\lambda_4$  are tunable hyperparameters. Note that during the second-phase training, we froze the parameters of the representation module  $\phi$  and the decoder network  $\psi$ , while train the representation adapter module  $\phi^U$  and the two prediction heads  $g_0, g_1$ . We summarize the whole learning algorithm in Alg. 1.

Compared to residual correction methods as in Kallus et al. [23], our representation adapter module guarantees a stronger representation ability, relaxing the linearly additive assumption. More importantly, when RCT data are limited, our proposed partial initialization strategy in the TSPF framework can avoid overfitting.

## 4 Experiment

### 4.1 Datasets

Following previous studies [33, 37, 45], we conduct experiments on two semi-synthetic datasets, namely **IHDP** [16] and **Jobs** [37]. The **IHDP** is a semi-synthetic dataset for causal effect estimation. The dataset is based on the Infant Health and Development Program, where the covariates are obtained by a randomized experiment investigating the effect of home visits by specialists on future cognitive scores. It consists of 747 units (19% treated, 81% control) and 25 covariates measuring the children and their mothers. The **Jobs** is a common benchmark dataset developed by LaLonde in 1986, studying the change of income and employment status after job training. We use an extended version of **Jobs** that comprises about 3,000 units (10% treated, 90% control) with 17 covariates.

### 4.2 Data Preprocessing

For both **IHDP** and **Jobs**, we simulate hidden confounding by generating a  $c$ -dimensional confounder  $U_i \in \mathbb{R}^c$ . To make sure the  $U_i$  has a non-zero effect on  $Y_i$  and  $T_i$ , we generate the data below:

$$\begin{aligned} W_1 &\sim \mathcal{N}(0, 0.1)^d, W_2 \sim \mathcal{N}(0.02, 0.1)^c, W_3 \sim \mathcal{N}(0.1, 1)^d, \\ W_4 &\sim \mathcal{N}(0.1, 1)^c, W_5 \sim \mathcal{U}(0, 0.2)^d, W_6 \sim \mathcal{U}(0, 0.2)^c, \\ U_i &\sim \mathcal{U}(0, 0.2)^c, T_i \sim \text{Bern}(\sigma(W_1 \cdot X_i + W_2 \cdot U_i)), \\ \mu_i^0 &= W_3 \cdot X_i + W_4 \cdot U_i, \mu_i^1 = W_5 \cdot X_i + W_6 \cdot U_i + 4, \\ Y_i^0 &\sim \mathcal{N}(\mu_i^0, 0.1), Y_i^1 \sim \mathcal{N}(\mu_i^1, 0.1), \end{aligned}$$

where  $\mathcal{N}(\mu, D)$  denotes the normal distribution with mean  $\mu$  and variance  $D$ ,  $\mathcal{U}(a, b)$  is the uniform distribution on interval  $(a, b)$ ,  $\text{Bern}(p)$  means the Bernoulli distribution with probability  $p$ ,  $\sigma(x) = 1/(1 + \exp(-x))$  is the sigmoid function. Note that we keep  $E[Y_i^1] = E[Y_i^0] + 4$  as the same as the **IHDP** dataset and we let  $E[W_i] > 0, i \in \{2, 4, 6\}$  to ensure the non-zero effect of  $U_i$ . The hidden confounding strength parameter  $c$  is set to 30 in our experiments. Then we slice the training, validation, and test sets in the ratio of 63/27/10. In addition, to obtain a separate RCT training dataset for data fusion, we first randomly split 10% of the training samples, and then assign treatments  $T_i^{new}$  according to the following formula and replace the factual treatment  $T_i$  and outcome  $Y_i^f$  to obtain a RCT dataset:

$$T_i^{new} = \text{Bern}(0.5), Y_i^{new} = \mathbb{I}\{T_i^{new} = T_i\}(Y_i^f - Y_i^{cf}) + Y_i^{cf},$$

where  $\mathbb{I}$  is the indicator function,  $Y_i^f = T_i Y_i^1 + (1 - T_i) Y_i^0$  is the factual outcome, and  $Y_i^{cf} = T_i Y_i^0 + (1 - T_i) Y_i^1$  is the counterfactual outcome. Finally, we replace the treatment  $T_i$  and factual outcome  $Y_i$  using the above formula for all samples in the validation set.

### 4.3 Baselines and Evaluation Metrics

#### 4.3.1 Baselines.

- T-learner [26]: T-learner utilizes two separate regressors for each treatment group.
- S-learner [1]: S-learner treats the indicator of treatment as features, utilizing a single model to estimate the potential outcome for both treatment and control groups.
- DR-learner [24]: DR-learner estimates the CATE via cross-fitting a doubly robust score function in two stages.

**Table 1: The experiment results on the IHDP dataset and Jobs dataset. The best result is bolded and the second best is underlined.**

Methods	IHDP				Jobs			
	In-sample		Out-sample		In-sample		Out-sample	
	$\sqrt{\epsilon_{PEHE}}$	$\epsilon_{ATE}$	$\sqrt{\epsilon_{PEHE}}$	$\epsilon_{ATE}$	$\sqrt{\epsilon_{PEHE}}$	$\epsilon_{ATE}$	$\sqrt{\epsilon_{PEHE}}$	$\epsilon_{ATE}$
T-learner	0.44 ± 0.03	0.04 ± 0.02	0.52 ± 0.05	<b>0.02 ± 0.01</b>	0.66 ± 0.27	<u>0.02 ± 0.02</u>	0.60 ± 0.20	<u>0.02 ± 0.01</u>
S-learner	0.98 ± 0.18	0.04 ± 0.03	1.37 ± 0.34	0.15 ± 0.10	0.70 ± 0.30	<u>0.02 ± 0.02</u>	0.67 ± 0.39	0.03 ± 0.02
DR-learner	0.71 ± 0.19	0.06 ± 0.04	0.81 ± 0.25	0.06 ± 0.03	0.50 ± 0.07	0.07 ± 0.02	0.48 ± 0.09	0.07 ± 0.03
SCIGAN	2.53 ± 0.47	0.63 ± 0.29	2.58 ± 0.57	0.55 ± 0.48	2.28 ± 0.75	0.56 ± 0.15	2.15 ± 0.80	0.47 ± 0.21
Causal Forest	1.90 ± 0.29	0.07 ± 0.05	2.04 ± 0.42	0.19 ± 0.11	1.38 ± 0.40	0.13 ± 0.08	1.23 ± 0.35	0.14 ± 0.08
TARNet	0.42 ± 0.09	0.05 ± 0.04	0.44 ± 0.12	0.05 ± 0.05	0.19 ± 0.17	<u>0.02 ± 0.01</u>	0.13 ± 0.02	<u>0.02 ± 0.01</u>
DragonNet	<u>0.19 ± 0.04</u>	<u>0.03 ± 0.02</u>	<u>0.26 ± 0.08</u>	<u>0.04 ± 0.02</u>	<u>0.15 ± 0.11</u>	<b>0.01 ± 0.01</b>	<u>0.11 ± 0.03</u>	<b>0.01 ± 0.01</b>
DESCN	0.28 ± 0.06	0.05 ± 0.05	0.41 ± 0.11	0.07 ± 0.06	0.44 ± 0.09	0.28 ± 0.13	0.44 ± 0.08	0.27 ± 0.13
DRCFR	0.74 ± 0.32	0.15 ± 0.10	0.90 ± 0.52	0.18 ± 0.17	0.91 ± 0.49	0.08 ± 0.08	0.71 ± 0.43	0.09 ± 0.07
CorNet	0.74 ± 0.32	0.15 ± 0.10	0.90 ± 0.52	0.18 ± 0.17	0.91 ± 0.49	0.08 ± 0.08	0.71 ± 0.43	0.09 ± 0.07
TSFP (ours)	<b>0.13 ± 0.02</b>	<b>0.02 ± 0.02</b>	<b>0.16 ± 0.04</b>	<u>0.04 ± 0.02</u>	<b>0.09 ± 0.03</b>	<b>0.01 ± 0.01</b>	<b>0.06 ± 0.01</b>	<b>0.01 ± 0.01</b>

- SCIGAN [45]: SCIGAN utilizes a generative adversarial network to model treatment effect.
- Causal Forest [39]: Causal Forest is a random forest-based model that directly estimates the treatment effect.
- TARNet [37]: TARNet applies a shared representation layer and a two-head network inference layer.
- DragonNet [38]: DragonNet designs an adaptive neural network to learn propensities and counterfactual outcomes.
- DESCN [48]: DESCN uses deep networks to model treatment effects in the entire sample space.
- DRCFR [12]: DRCFR aims to learn disentangled representations of covariates and address selection bias in CATE estimation.
- CorNet [13]: CorNet leverages OBS data to learn a biased estimate for the treatment effect and then aims to estimate the non-linear bias using RCT data.

4.3.2 *Evaluation Metrics.* Following previous studies [37, 44], we evaluate the performance of CATE estimation using *the square root of Precision in Estimation of Heterogeneous Effects* (PEHE):

$$\sqrt{\epsilon_{PEHE}} = \sqrt{\frac{1}{n} \sum_{i=1}^n ((\hat{Y}_i^1 - \hat{Y}_i^0) - (Y_i^1 - Y_i^0))^2},$$

where  $\hat{Y}_i^t$  and  $Y_i^t$  are the predicted and ground truth values for the potential outcomes of individual  $i$  under treatment  $t$ . In addition, we also use the *absolute error in Average Treatment Effect* (ATE) to evaluate estimation performance, which is defined as:

$$\epsilon_{ATE} = \frac{1}{n} \left| \sum_{i=1}^n ((\hat{Y}_i^1 - \hat{Y}_i^0) - (Y_i^1 - Y_i^0)) \right|.$$

4.3.3 *Experimental Details.* We adopt a multi-layer perceptron [15] with 2 layers for our representation and reconstruction modules as well as the prediction heads in both stages. We tune the scale parameters in the loss functions from  $1e-5$  to 0.1. For the baselines with only one stage, we combine the OBS and RCT samples as

the training dataset. We report both in-sample and out-of-sample results for  $\sqrt{\epsilon_{PEHE}}$  and  $\epsilon_{ATE}$  metrics in our experiments.

#### 4.4 Performance Analysis

Table 1 shows the prediction performance with varying baselines and our methods. First, representation-based methods generally outperform generation-based methods and meta-learners, which shows the effectiveness of causal representation learning. Note that our TSFP exhibits the most competitive performance in most cases, outperforming both the representation-based and generation-based methods. More importantly, TSFP significantly outperforms another two-stage method CorNet for all metrics on the two datasets.

### 5 Conclusion

This paper studies the CATE estimation problem in the presence of hidden confounding for fusing large-scale OBS data and small-scale RCT data. We propose a two-stage pretraining-finetuning framework to tackle the overfitting problem caused by the small-scale RCT data. Specifically, the foundational representation learned in the first stage is used to adjust for the *measured* confounding bias in the OBS data. The augmented representation learned in the second stage is used to mitigate for the *hidden* confounding bias guided by the RCT data. To avoid overfitting caused by the small-scale RCT data in the second stage, instead of training a separate network, we propose to partially initialize the network parameters from the pretrained network from the first stage. Compared to the previous CATE estimation methods that combine OBS and RCT data, our approach has the advantage of not restricting the data-generating process (e.g., linearity or additive noise assumptions) and suffering from overfitting. The experiments conducted in the real-world datasets demonstrate the superiority of our approach.

### Acknowledgments

HL was supported by National Natural Science Foundation of China (623B2002). MG was supported by ARC DE210101624 and ARC DP240102088.

## References

- [1] Susan Athey and Guido W Imbens. 2015. Machine learning methods for estimating heterogeneous causal effects. *Stat* 1050, 5 (2015), 1–26.
- [2] Florent Bédécarrats, Isabelle Guérin, and François Roubaud. 2020. *Randomized control trials in the field of development: A critical perspective*. Oxford University Press.
- [3] Diogo GC Britto, Paolo Pinotti, and Breno Sampaio. 2022. The effect of job loss and unemployment insurance on crime in Brazil. *Econometrica* 90, 4 (2022), 1393–1423.
- [4] Marie-Laure Charpignon, Bella Vakulenko-Lagun, Bang Zheng, Colin Magdamo, Bowen Su, Kyle Evans, Steve Rodriguez, Artem Sokolov, Sarah Boswell, Yi-Han Sheu, et al. 2022. Causal inference in medical records and complementary systems pharmacology for metformin drug repurposing towards dementia. *Nature Communications* 13, 1 (2022), 7652.
- [5] Pengyu Cheng, Weituo Hao, Shuyang Dai, Jiachang Liu, Zhe Gan, and Lawrence Carin. 2020. Club: A contrastive log-ratio upper bound of mutual information. In *International Conference on Machine Learning*. PMLR, 1779–1788.
- [6] Bénédicte Colnet, Imke Mayer, Guanhua Chen, Awa Dieng, Ruohong Li, Gaël Varoquaux, Jean-Philippe Vert, Julie Josse, and Shu Yang. 2024. Causal inference methods for combining randomized trials and observational studies: a review. *Statist. Sci.* 39, 1 (2024), 165–191.
- [7] Giovanni Corrao, Federica Nicotra, Andrea Parodi, Antonella Zambon, Davide Soranna, Franca Heiman, Luca Merlino, and Giuseppe Mancina. 2012. External adjustment for unmeasured confounders improved drug–outcome association estimates based on health care utilization data. *Journal of Clinical Epidemiology* 65, 11 (2012), 1190–1199.
- [8] Jacob Dorn, Kevin Guo, and Nathan Kallus. 2024. Doubly-valid/doubly-sharp sensitivity analysis for causal inference with unmeasured confounding. *J. Amer. Statist. Assoc.* (2024), 1–12.
- [9] Charlie Frogner, Chiyuan Zhang, Hossein Mobahi, Mauricio Araya, and Tomaso A Poggio. 2015. Learning with a Wasserstein loss. *Advances in Neural Information Processing Systems* 28 (2015).
- [10] Isabel R Fulcher, Ilya Shpitser, Stella Marealle, and Eric J Tchetgen Tchetgen. 2020. Robust inference on population indirect causal effects: the generalized front door criterion. *Journal of the Royal Statistical Society Series B: Statistical Methodology* 82, 1 (2020), 199–214.
- [11] Fernando Pires Hartwig, Linbo Wang, George Davey Smith, and Neil Martin Davies. 2023. Average causal effect estimation via instrumental variables: the no simultaneous heterogeneity assumption. *Epidemiology* 34, 3 (2023), 325–332.
- [12] Negar Hassanpour and Russell Greiner. 2019. Learning disentangled representations for counterfactual regression. In *International Conference on Learning Representations*.
- [13] Tobias Hatt, Jeroen Berrevoets, Alicia Curth, Stefan Feuerriegel, and Mihaela van der Schaar. 2022. Combining observational and randomized data for estimating heterogeneous treatment effects. *arXiv:2202.12891* (2022).
- [14] Tobias Hatt, Daniel Tschernutter, and Stefan Feuerriegel. 2022. Generalizing off-policy learning under sample selection bias. In *Uncertainty in Artificial Intelligence*. PMLR, 769–779.
- [15] Simon Haykin. 1994. *Neural Networks: A Comprehensive Foundation*. Macmillan.
- [16] Jennifer L Hill. 2011. Bayesian nonparametric modeling for causal inference. *Journal of Computational and Graphical Statistics* 20, 1 (2011), 217–240.
- [17] Jeroen Hoogland, Joanna Int’Hout, Michail Belias, Maroeska M Rovers, Richard D Riley, Frank E. Harrell Jr, Karel GM Moons, Thomas PA Debray, and Johannes B Reitsma. 2021. A tutorial on individualized treatment effect prediction from randomized trials with a binary endpoint. *Statistics in Medicine* 40, 26 (2021), 5961–5981.
- [18] Van-Nam Huynh, Vladik Kreinovich, and Songsak Sriboonchitta. 2016. *Causal inference in econometrics*. Springer.
- [19] Guido W Imbens. 2003. Sensitivity to exogeneity assumptions in program evaluation. *American Economic Review* 93, 2 (2003), 126–132.
- [20] Guido W Imbens and Donald B Rubin. 2015. *Causal inference in statistics, social, and biomedical sciences*. Cambridge university press.
- [21] Fredrik Johansson, Uri Shalit, and David Sontag. 2016. Learning representations for counterfactual inference. In *International Conference on Machine Learning*. PMLR, 3020–3029.
- [22] Guido W. Imbens Joshua D. Angrist and Donald B. Rubin. 1996. Identification of Causal Effects Using Instrumental Variables. *J. Amer. Statist. Assoc.* 91, 434 (1996), 444–455.
- [23] Nathan Kallus, Aahlad Manas Puli, and Uri Shalit. 2018. Removing hidden confounding by experimental grounding. *Advances in Neural Information Processing Systems* 31 (2018).
- [24] Edward H. Kennedy. 2023. Towards optimal doubly robust estimation of heterogeneous causal effects. *Electronic Journal of Statistics* 17, 2 (2023), 3008 – 3049. <https://doi.org/10.1214/23-EJS2157>
- [25] Lingjing Kong, Guangyi Chen, Petar Stojanov, Haoxuan Li, Eric P Xing, and Kun Zhang. 2025. Towards Understanding Extrapolation: a Causal Lens. *Advances in Neural Information Processing Systems* 37 (2025).
- [26] Sören R Künzel, Jasjeet S Sekhon, Peter J Bickel, and Bin Yu. 2019. Metalearners for estimating heterogeneous treatment effects using machine learning. *Proceedings of the National Academy of Sciences* 116, 10 (2019), 4156–4165.
- [27] Baohong Li, Haoxuan Li, Anpeng Wu, Minqin Zhu, Qingyu Cao, and Kun Kuang. 2024. A Generative Approach for Treatment Effect Estimation under Collider Bias: From an Out-of-Distribution Perspective. In *International Conference on Machine Learning*. PMLR.
- [28] Baohong Li, Haoxuan Li, Ruoxuan Xiong, Anpeng Wu, Fei Wu, and Kun Kuang. 2024. Learning Shadow Variable Representation for Treatment Effect Estimation under Collider Bias. In *International Conference on Machine Learning*. PMLR.
- [29] Haoxuan Li, Kunhan Wu, Chunyuan Zheng, Yanghao Xiao, Hao Wang, Zhi Geng, Fuli Feng, Xiangnan He, and Peng Wu. 2024. Removing hidden confounding in recommendation: a unified multi-task learning approach. *Advances in Neural Information Processing Systems* 36 (2024).
- [30] Haoxuan Li, Yanghao Xiao, Chunyuan Zheng, and Peng Wu. 2023. Balancing unobserved confounding with a few unbiased ratings in debiased recommendations. In *Proceedings of the ACM Web Conference 2023*. 1305–1313.
- [31] Haoxuan Li, Chunyuan Zheng, Yixiao Cao, Zhi Geng, Yue Liu, and Peng Wu. 2023. Trustworthy policy learning under the counterfactual no-harm criterion. In *International Conference on Machine Learning*. PMLR, 20575–20598.
- [32] Xitong Li, Jörn Grahl, and Oliver Hinz. 2022. How do recommender systems lead to consumer purchases? A causal mediation analysis of a field experiment. *Information Systems Research* 33, 2 (2022), 620–637.
- [33] Christos Louizos, Uri Shalit, Joris M Mooij, David Sontag, Richard Zemel, and Max Welling. 2017. Causal effect inference with deep latent-variable models. *Advances in Neural Information Processing Systems* 30 (2017).
- [34] Judea Pearl. 2009. *Causality*. Cambridge university press.
- [35] Mattia Proserpi, Yi Guo, Matt Sperrin, James S Koopman, Jae S Min, Xing He, Shannan Rich, Mo Wang, Iain E Buchan, and Jiang Bian. 2020. Causal inference and counterfactual prediction in machine learning for actionable healthcare. *Nature Machine Intelligence* 2, 7 (2020), 369–375.
- [36] JAMES M Robins and MA Hernán. 2016. Causal inference.
- [37] Uri Shalit, Fredrik D Johansson, and David Sontag. 2017. Estimating individual treatment effect: generalization bounds and algorithms. In *International Conference on Machine Learning*. PMLR, 3076–3085.
- [38] Claudia Shi, David Blei, and Victor Veitch. 2019. Adapting neural networks for the estimation of treatment effects. *Advances in neural information processing systems* 32 (2019).
- [39] Stefan Wager and Susan Athey. 2018. Estimation and inference of heterogeneous treatment effects using random forests. *J. Amer. Statist. Assoc.* 113, 523 (2018), 1228–1242.
- [40] Hao Wang, Jiajun Fan, Zhichao Chen, Haoxuan Li, Weiming Liu, Tianqiao Liu, Quanyu Dai, Yichao Wang, Zhenhua Dong, and Ruiming Tang. 2024. Optimal transport for treatment effect estimation. *Advances in Neural Information Processing Systems* 36 (2024).
- [41] Lili Wu and Shu Yang. 2022. Integrative R-learner of heterogeneous treatment effects combining experimental and observational studies. In *Conference on Causal Learning and Reasoning*. PMLR, 904–926.
- [42] Peng Wu, Haoxuan Li, Yuhao Deng, Wenjie Hu, Quanyu Dai, Zhenhua Dong, Jie Sun, Rui Zhang, and Xiao-Hua Zhou. 2022. On the Opportunity of Causal Learning in Recommendation Systems: Foundation, Estimation, Prediction and Challenges. In *International Joint Conference on Artificial Intelligence*. Survey Track.
- [43] Yunfu Xu and Aiyi Li. 2020. The relationship between innovative human capital and interprovincial economic growth based on panel data model and spatial econometrics. *J. Comput. Appl. Math.* 365 (2020), 112381.
- [44] Liuyi Yao, Sheng Li, Yaliang Li, Mengdi Huai, Jing Gao, and Aidong Zhang. 2018. Representation learning for treatment effect estimation from observational data. *Advances in Neural Information Processing Systems* 31 (2018).
- [45] Jinsung Yoon, James Jordon, and Mihaela Van Der Schaar. 2018. GANITE: Estimation of individualized treatment effects using generative adversarial nets. In *International Conference on Learning Representations*.
- [46] Emily C Zabor, Alexander M Kaizer, and Brian P Hobbs. 2020. Randomized controlled trials. *Chest* 158, 1 (2020), S79–S87.
- [47] Yao Zhang, Alexis Bellot, and Mihaela Schaar. 2020. Learning overlapping representations for the estimation of individualized treatment effects. In *International Conference on Artificial Intelligence and Statistics*. PMLR, 1005–1014.
- [48] Kailiang Zhong, Fengtong Xiao, Yan Ren, Yaorong Liang, Wenqing Yao, Xiaofeng Yang, and Ling Cen. 2022. Descn: Deep entire space cross networks for individual treatment effect estimation. In *Proceedings of the 28th ACM SIGKDD Conference on Knowledge Discovery and Data Mining*. 4612–4620.
- [49] Minqin Zhu, Anpeng Wu, Haoxuan Li, Ruoxuan Xiong, Bo Li, Xiaoqing Yang, Xuan Qin, Peng Zhen, Jiecheng Guo, Fei Wu, and Kun Kuang. 2024. Contrastive balancing representation learning for heterogeneous dose-response curves estimation. In *Proceedings of the AAAI Conference on Artificial Intelligence*, Vol. 38. 17175–17183.